KAPL-P-000081
(K98071)
CONF-9805146--

IN-SITU MONITORING OF GaSb, GaInAsSb, and AlGaAsSb

C. J. Vineis, C. A. Wang, K. F. Jensen, W. G. Breiland

June 1998

NOTICE

KAPL ATOMIC POWER LABORATORY SCHENECTADY, NEW YORK 12301

Operated for the U. S. Department of Energy
by KAPL, Inc. a Lockheed Martin company

DISCLAIMER

In-Situ Monitoring of GaSb, GaInAsSb, and AlGaAsSb*

C.J. Vineis[1,2,†], C.A.Wang[1], K.F. Jensen[2,3], and W.G. Breiland[4]
[1]Lincoln Laboratory, Massachusetts Institute of Technology, Lexington, MA 02173-9108
[2]Dept. of Materials Science and Engineering, Massachusetts Institute of Technology, Cambridge, MA 02139-4307
[3]Dept. of Chemical Engineering, Massachusetts Institute of Technology, Cambridge, MA 02139-4307
[4]Sandia National Laboratories, Albuquerque, New Mexico 87185-0601

Abstract

Suitability of silicon photodiode detector arrays for monitoring the spectral reflectance during epitaxial growth of GaSb, AlGaAsSb, and GaInAsSb, which have cutoff wavelengths of 1.7, 1.2, and 2.3 μm, respectively, is demonstrated. These alloys were grown lattice matched to GaSb in a vertical rotating-disk reactor, which was modified to accommodate near normal reflectance without affecting epilayer uniformity. By using a virtual interface model, the growth rate and complex refractive index at the growth temperature are extracted for these alloys over the 600 to 950 nm spectral range. Excellent agreement is obtained between the extracted growth rate and that determined by ex-situ measurement. Optical constants are compared to theoretical predictions based on an existing dielectric function model for these materials. Furthermore, quantitative analysis of the entire reflectance spectrum yields valuable information on the approximate thickness of overlayers on the pregrowth substrate.

*This work was sponsored by the Department of Energy under AF Contract No. F19628-95-C-0002. The opinions, interpretations, conclusions and recommendations are those of the author and are not necessarily endorsed by the United States Air Force.
† email: cjv@ll.mit.edu

1. Introduction

In-situ optical monitoring during organometallic vapor phase epitaxy (OMVPE) provides insight into complex growth processes, and has led to improvements in the growth process and the resulting materials. Techniques for monitoring the epitaxial growth include spectral reflectance (SR), thermal emission, spectroscopic ellipsometry (SE), reflectance difference spectroscopy (RDS), and surface photoabsorption [1]. Each of these optical probes is sensitive to different properties of a material, and thus could be used simultaneously to obtain complementary information during epitaxial growth. For example, RDS has been demonstrated to be a useful method for monitoring surface processes [2], while SE enables accurate determination of thin film refractive indices and thicknesses [3], and SR yields real-time information on the growth rate and complex refractive index [4].

Near-normal SR is a particularly attractive technique for in-situ monitoring because it provides information that can be quickly analyzed for closed-loop process control [5], and is less expensive and easier to implement than most other in-situ process monitors. It has been demonstrated as a useful tool for in-situ monitoring of OMVPE III-V arsenides [4-6], phosphides [7,8], and nitrides [9]. For those materials systems, Si detectors were used. However, since antimonide-based alloys have smaller bandgaps and higher absorption over the Si wavelength range (typically 400-1100 nm), it is not apparent whether Si detectors would be acceptable for monitoring the growth of antimonide-based materials. Previous work in InP-based materials indicated that absorption was significant in the wavelength range of the silicon detector, and improved results were obtained by using a PbS detector to extend the wavelength range to 2500 nm [7,8].

Since it is desirable to use off-the-shelf, readily available components to maintain low costs, we investigated the usefulness of a conventional Si photodiode array (PDA) for monitoring in-situ the SR during growth of III-V antimonide-based materials. We demonstrate that a Si PDA can provide sufficient SR for GaSb, AlGaAsSb, and GaInAsSb. Extracted growth rates compare favorably with layer thicknesses determined ex-situ using double crystal x-ray diffraction (DCXD). Information obtained from quantitative analysis of the entire reflectance spectrum is discussed, and optical constants at the growth temperature are presented in terms of an existing dielectric function model [10, 11].

2. Experimental procedure and reactor development

Figure 1 shows a schematic diagram of the experimental setup. Optical fibers are used to direct white light from a 5 W tungsten halogen lamp to the vertical rotating-disk reactor, and the reflected signal to the Si PDA spectrometer, which interfaces directly to the computer. The Si spectrometer is a commercial 512 element array with a wavelength range of 380 to 1100 nm and 2.4 nm resolution. Integration times as low as 10 ms may be used to acquire spectra, although for our growth rates a one second integration time was sufficient. The unit is compact and entirely contained on a PC card that plugs directly into a computer expansion slot. The spectral response as a function of growth time was acquired via a Windows-based program and stored to disk. Quantitative analysis of the reflectance was performed using a virtual interface model [4] to yield the growth rate and complex refractive index.

The vertical rotating-disk reactor utilizes a mesh screen to ensure plug flow into the reactor [12], and was modified to incorporate an optical window at the center of the mesh. The diameter of the optical window is constrained by epitaxial growth nonuniformities and heterostructure

grading that could occur if the unswept volume below the window is too large. In order to assess the effects of window diameter on growth, numerical simulations of the flow and temperature fields were performed for the reactor under typical growth conditions: 10-cm-diam quartz tube, 15 cm inlet-to-susceptor distance, 10 slpm H_2 carrier flow rate, 150 Torr reactor pressure, 650°C susceptor temperature, and 400 rpm susceptor rotation rate. The window radius was either 1.25 or 2.54 cm. For the 1.25-cm-radius window, shown in Fig. 2a, the gas sweeps out the volume below the window with minimal change in temperature and flow fields compared to those computed without the window [12]. Consequently, the epitaxial growth characteristics are preserved. When the window radius is increased to 2.54 cm, shown in Fig. 2b, gas expansion results in a recirculation below the window which can lead to heterostructures with graded interfaces. Because of high gas diffusivity, layer uniformity is unaffected by the larger optical window. The optical window used in these experiments has a 1.1 cm radius.

GaSb, GaInAsSb, and AlGaAsSb epilayers were grown in a vertical rotating-disk reactor with H_2 carrier gas at a flow rate of 10 slpm and reactor pressure of 150 Torr, as described previously [13]. Triethylgallium, trimethylindium, tritertiarybutylaluminum, trimethylantimony, and tertiarybutylarsine were used as precursors. Layers were grown at 525 or 550°C on Te-doped GaSb or semi-insulating GaAs substrates, (100) misoriented 6° toward (111)B. Epitaxial layer thickness was determined by using DCXD.

3. Results and discussion

3.1 Growth rates and optical constants

Figure 3 shows the SR as a function of time at 800 nm for the following layers grown lattice matched to a GaSb substrate: GaSb buffer layer, AlGaAsSb, GaSb, GaInAsSb, and GaSb. The cutoff wavelength λ at 25°C of the GaSb, AlGaAsSb, and GaInAsSb is 1.7, 1.2, and 2.2 μm,

respectively. The beginning of each layer is indicated in the figure. The SR is characterized by small amplitude, high frequency oscillations superimposed on larger amplitude, smaller frequency oscillations related to epilayer growth. The small amplitude, high frequency oscillations are noise resulting from wobble of the rotating wafer.

Quantitative analysis of the SR requires a minimum degree of transparency of the growing layer. Ideally, at least one full period should exist for accurate curve fitting analysis. However, because absorption becomes significant for wavelengths much smaller than the bandgap of the layer, the oscillation amplitude decreases with increasing growth time. Figure 3 confirms that for a wavelength of 800 nm, at least one oscillation occurs before the onset of significant absorption in all three materials, indicating that Si photodiode arrays are suitable for monitoring the growth of these III-V antimonides.

Figure 4 shows the SR at 550 and 850 nm as a function of time for GaSb grown lattice mismatched on a GaAs substrate. At 550 nm one period is 215 s long, while at 850 nm the period is 335 s. Oscillations in the reflectance damp out much more slowly at 850 nm than at 550 nm because of the lower absorption of GaSb at longer wavelengths. However, the larger oscillation period requires a longer growth time before the growth rate and optical constants can be accurately determined. These results show that the particular advantage of using SR instead of single wavelength reflectance is that various materials and layer structures are better monitored at different wavelengths. For example, it may be preferable to monitor the growth of thick layers at the longer wavelengths so the growth rate can be extracted for extended time periods. Alternatively, shorter wavelengths would be more appropriate for monitoring thin layers, such as quantum well structures.

The growth rate of GaInAsSb with λ ~ 2.3 μm, grown lattice matched to GaSb, was extracted using the virtual interface model [4] for several wavelengths between 600 and 850 nm. The results indicate a film thickness of 2875 Å ±200 Å , which compares extremely well to the actual thickness of 2832 Å determined by ex-situ DCXD. SR in the range of 750-850 nm gave thickness values within 5% of each other, while the error increased when shorter wavelengths were used. Another advantage of using SR over single wavelength reflectance is the over-determination of the film thickness which results in a more reliable value.

Figures 5 (a) and (b) show the extracted optical constants (n and k) at 550°C for GaSb grown on a GaAs substrate, and the theoretical values for unstrained GaSb at 550°C. Also shown are theoretical and experimental values [14] at 25°C. The theoretical values are based on a model dielectric function [10, 11, 15, 16] which calculates the imaginary component of the dielectric function ($\varepsilon_2(\omega)$, where $\varepsilon(\omega)=\varepsilon_1(\omega)-i*\varepsilon_2(\omega)$ is the complex dielectric constant), and then uses Kramers-Kronig analysis to determine the real part of the dielectric function. The complex refractive index is calculated from the complex dielectric function, and further calculations enable predictions of the reflectance and absorbance. The imaginary component of the dielectric function, $\varepsilon_2(\omega)$, is obtained by considering contributions from various critical points in the material (i.e., the various interband transitions: E_0, $E_0+\Delta_0$, E_1, $E_1+\Delta_1$, etc.). The effect of each critical point depends on three parameters: its size (bandgap), the strength of the transition, and the lifetime broadening of the transition. A powerful feature of this model is its ability to account for the effect of perturbations (such as temperature and strain) on the dielectric function. Theoretical reflectance spectra as a function of temperature for GaAs and GaSb are in good agreement with experimental results shown in Figs. 6 (a) and (b), providing confidence in the theoretical values of n and k shown in Figs. 5 (a) and (b).

The discrepancy between the extracted and theoretical optical constants at 550°C shown in Fig. 5 may be due to the 8% lattice mismatch between GaSb and GaAs. It is likely that the GaSb layer is relaxed and a high density of misfit dislocations are present at the interface. The effects of scattering at the interface as a result of misfit dislocations have not been included in the virtual interface model; therefore, those results should differ from values obtained for unstrained GaSb.

Figures 7 and 8 show the extracted optical constants for AlGaAsSb and GaInAsSb layers grown lattice matched to GaSb. In theory, refractive indices for ternaries and quaternaries can be obtained by combining the functions for the constituent binaries [Ref. 10, pp. 289-91]. Unfortunately, little information is available about the refractive indices of AlGaAsSb and GaInAsSb in the Si detector wavelength range (especially at the elevated growth temperatures). Therefore, comparison of our extracted data to literature values is not possible.

3.2 Oxide overlayers

SR can also be useful for determining the presence of overlayers on a substrate. Figure 9 compares theoretical SR for "clean" GaSb, GaSb with a 20 Å oxide layer, and GaSb with a 60 Å oxide layer. The oxide refractive index used for the calculations was taken from published data in references 17 and 18. Also shown in Fig. 9 is the SR for a GaSb substrate which had been etched and exposed to air for several days. The wavelength range of the Si detector array is well matched to detecting the presence of the oxide overlayer because the dielectric function is most sensitive to oxide overlayers at energies above the E_1 transition, which is about 600 nm in GaSb at 25°C [17]. For wavelengths with energies below this transition, the reflectance is barely affected by the presence of an oxide, and thus reflectance at longer wavelengths would not be suitable for this purpose. Curve fitting the measured SR to a GaSb substrate/thin oxide film/ambient model results in an oxide film thickness of about 50 Å, which is in good agreement

with typical ones of 50-60 Å determined for GaSb under similar conditions [17]. Since clean, oxide-free substrate surfaces are very important for high quality epitaxial growth, these results illustrate that quantitative analysis of the SR from the substrate before growth yields insight into the quality and consistency of the wafer preparation process.

4. Summary

Near-normal spectral reflectance using a Si photodiode array has been demonstrated as a useful tool for monitoring the growth of III-V antimonide-based alloys. Growth rates extracted from the reflectance signal at various wavelengths compare favorably with film thicknesses measured ex-situ using DCXD. Optical constants at the growth temperature of 550°C have also been extracted from the reflectance for GaSb, AlGaAsSb, and GaInAsSb; and the values for GaSb have been compared to theoretical predictions based on an existing dielectric function model. Furthermore, the usefulness of examining the SR as a tool for monitoring the quality of the pregrowth wafer preparation process has been discussed.

Acknowledgments

The authors gratefully acknowledge S.R. Chinn and D.L. Spears for helpful discussions; T.G. Mihopoulos for finite element calculations; D.C. Oakley, J.W. Chludzinski, and J.W. Caunt for assistance in experimental design and crystal growth; and D.R. Calawa for x-ray diffraction.

References

1. I. P. Herman, *Optical Diagnostics for Thin Film Processing*. Academic Press, New York, 1996.

2. D.E. Aspnes, IEEE J. Quantum Electron. 25 (1989) 1056.

3. E. A. Irene, Thin Solid Films 233 (1993) 96.

4. W. G. Breiland and K. P. Killeen, J. Appl. Phys. 78 (1995) 6726.

5. H. Sankur, W. Southwell, and R. Hall, J. Electron. Mater. 20 (1991) 1099.

6. N.C. Frateschi, S.G. Hummel, and P.D. Dapkus, Electron. Lett. 27 (1991) 155.

7. J. C. Bean, L. J. Peticolas, R. Lum, and M. L. McDonald, J. Vac. Sci. Technol. A 14 (1996) 946.

8. R. M. Lum, M. L. McDonald, J.C. Bean, J. Vandenberg, T. L. Pernell, S. N. G. Chu, A. Robertson, and A. Karp, Appl. Phys. Lett. 69 (1996) 928.

9. K. Killeen, M.J. Ludowise, W.H. Perez, S.D. Lester, Y-L. Chang, D. Lefforge, and J.N. Miller, 8th Biennial Workshop on Organometallic Vapor Phase Epitaxy, April 1997, Dana Point, CA.

10. S. Adachi, *Physical Properties of III-V Semiconductor Compounds*, John Wiley & Sons, New York, 1992, p. 135-193.

11. S. Adachi, J. Appl. Phys. 66 (1989) 6030.

12. C.A. Wang, S. Patnaik, J.W. Caunt, and R.A. Brown, J. Cryst. Growth 93 (1988) 228.

13. C.A. Wang, accepted J. Cryst. Growth.

14. Handbook of Optical Constants, ed. E.D. Palik, Acdemic Press, 1991.

15. S. Adachi, Phys. Rev. B 41 (1990) 1003.

16. S. Zollner, M. Garriga, J. Humlícek, S. Gopalan and M. Cardona, Phys. Rev. B 43 (1991) 4349.

17. D. E. Aspnes, B. Schwartz, A. A. Studna, L. Derick, and L. A. Koszi, J. Appl. Phys. 48 (1977) 3510.

18. S. Zollner, Appl. Phys. Lett. 63 (1993) 2523.

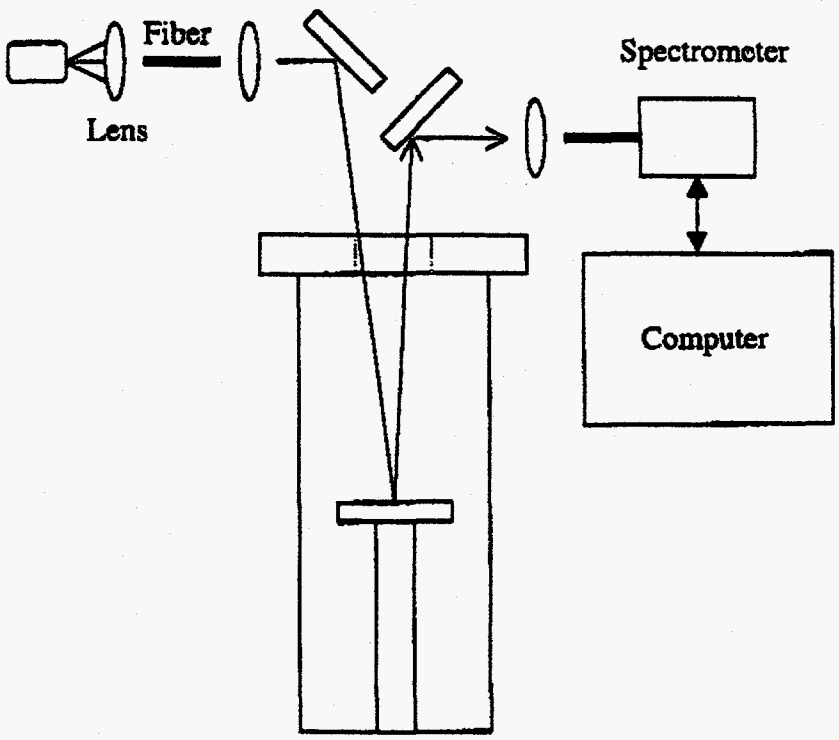

Figure 1. Schematic diagram of the experimental setup for in-situ process monitoring using near-normal spectral reflectance.

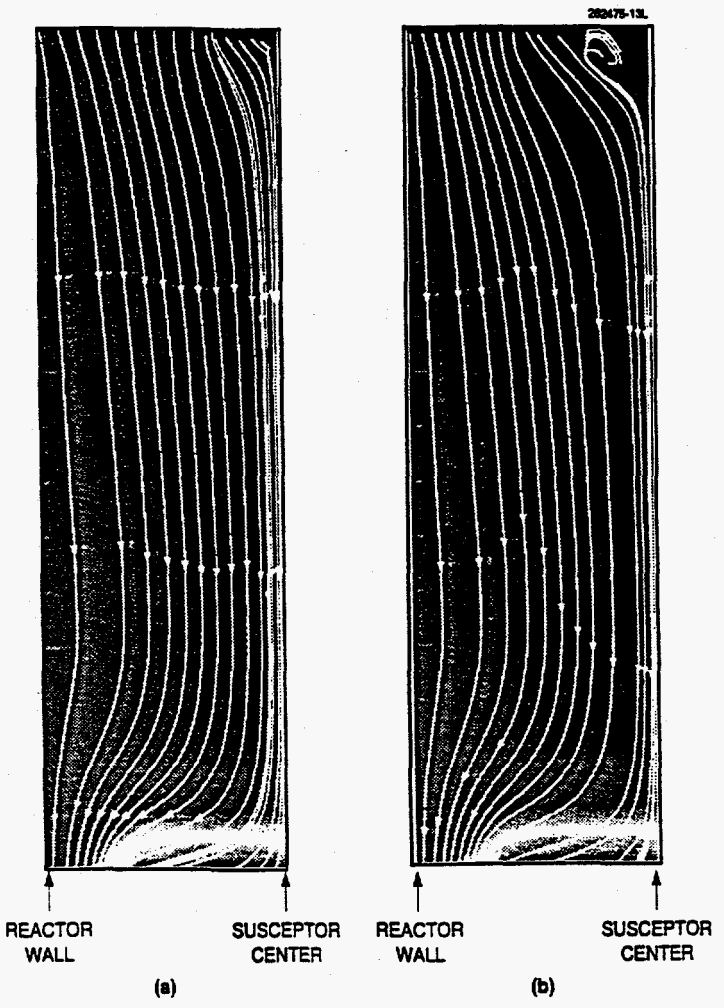

Figure 2. Flow patterns for (a) 1.25-cm-radius optical window and (b) 2.54-cm-radius optical window.

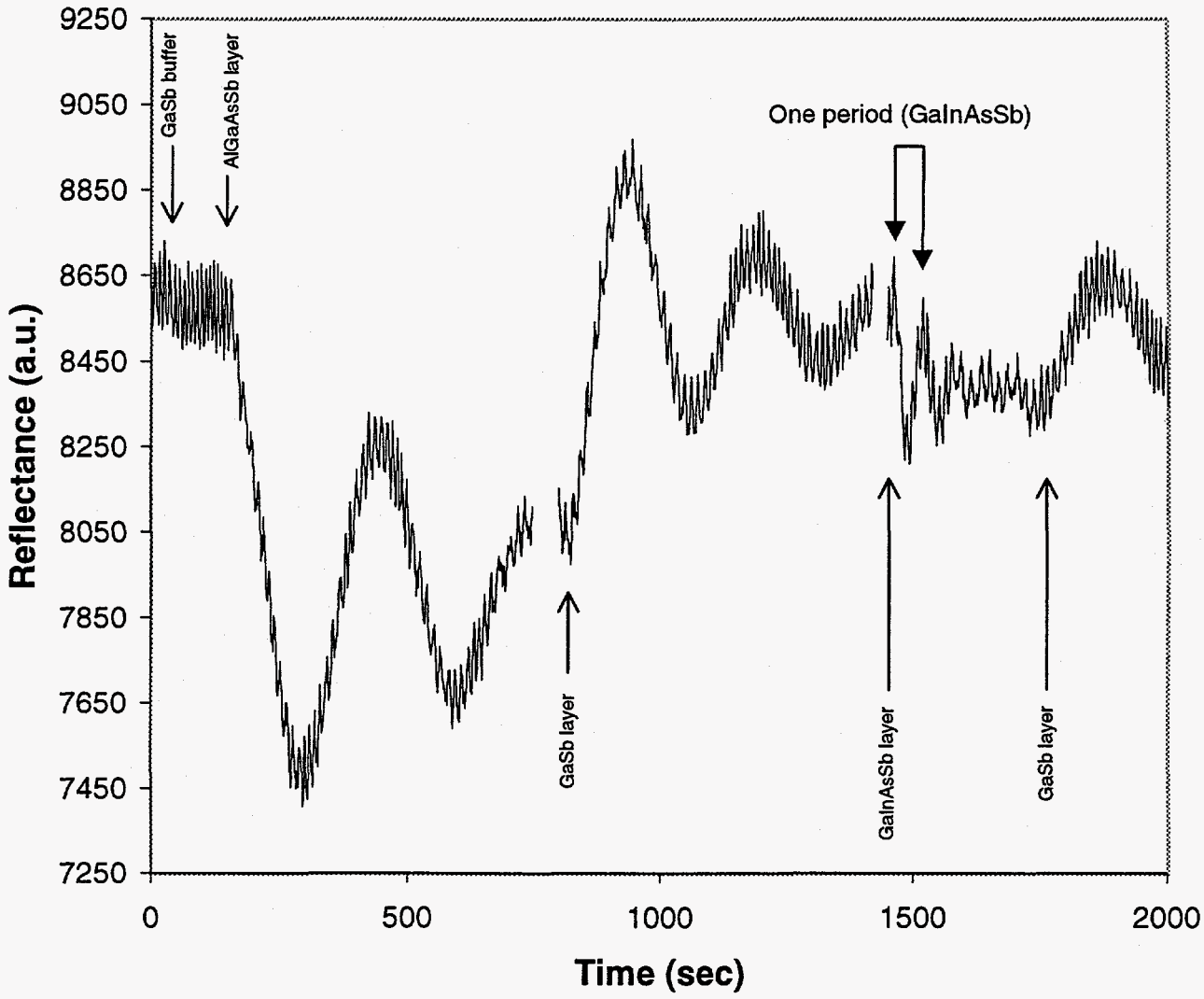

Figure 3. Reflectance at 800 nm of GaSb, AlGaAsSb, and GaInAsSb, on GaSb. (The noise in the signal is due to sample wobble.)

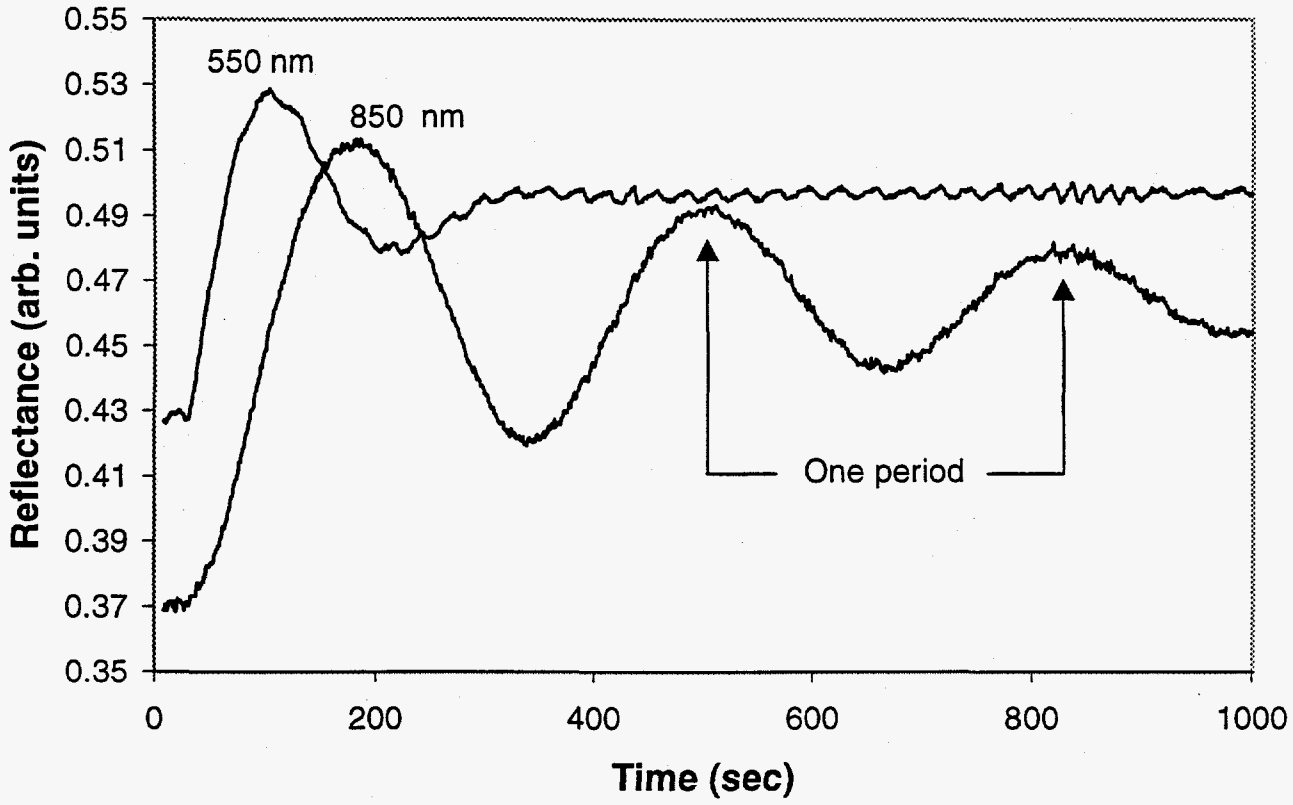

Figure 4. Reflectance at 850 nm and 550 nm of GaSb grown on GaAs. (The small amplitude, high frequency oscillations superimposed on the large amplitude oscillations are noise resulting from sample wobble during rotation.)

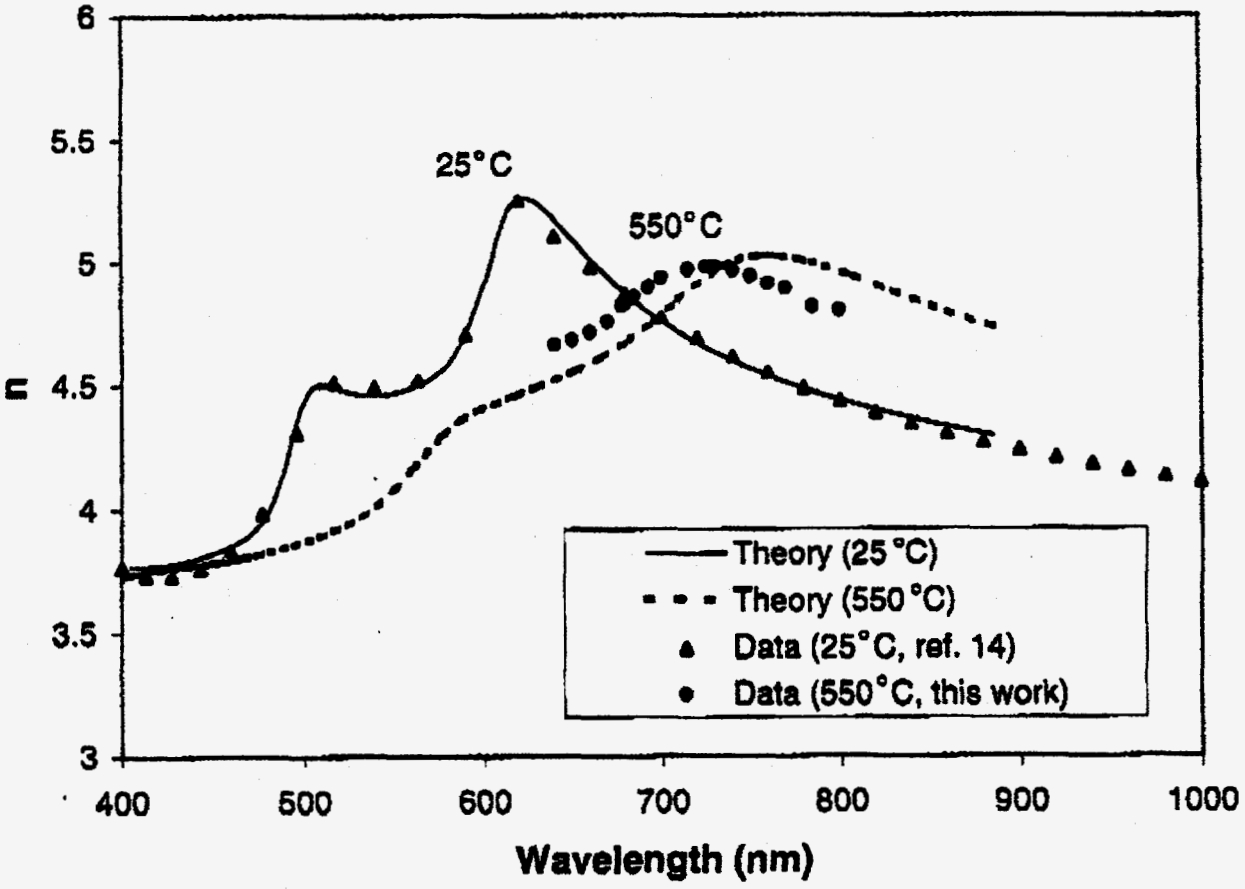

Figure 5(a). Real part of the refractive index for GaSb.

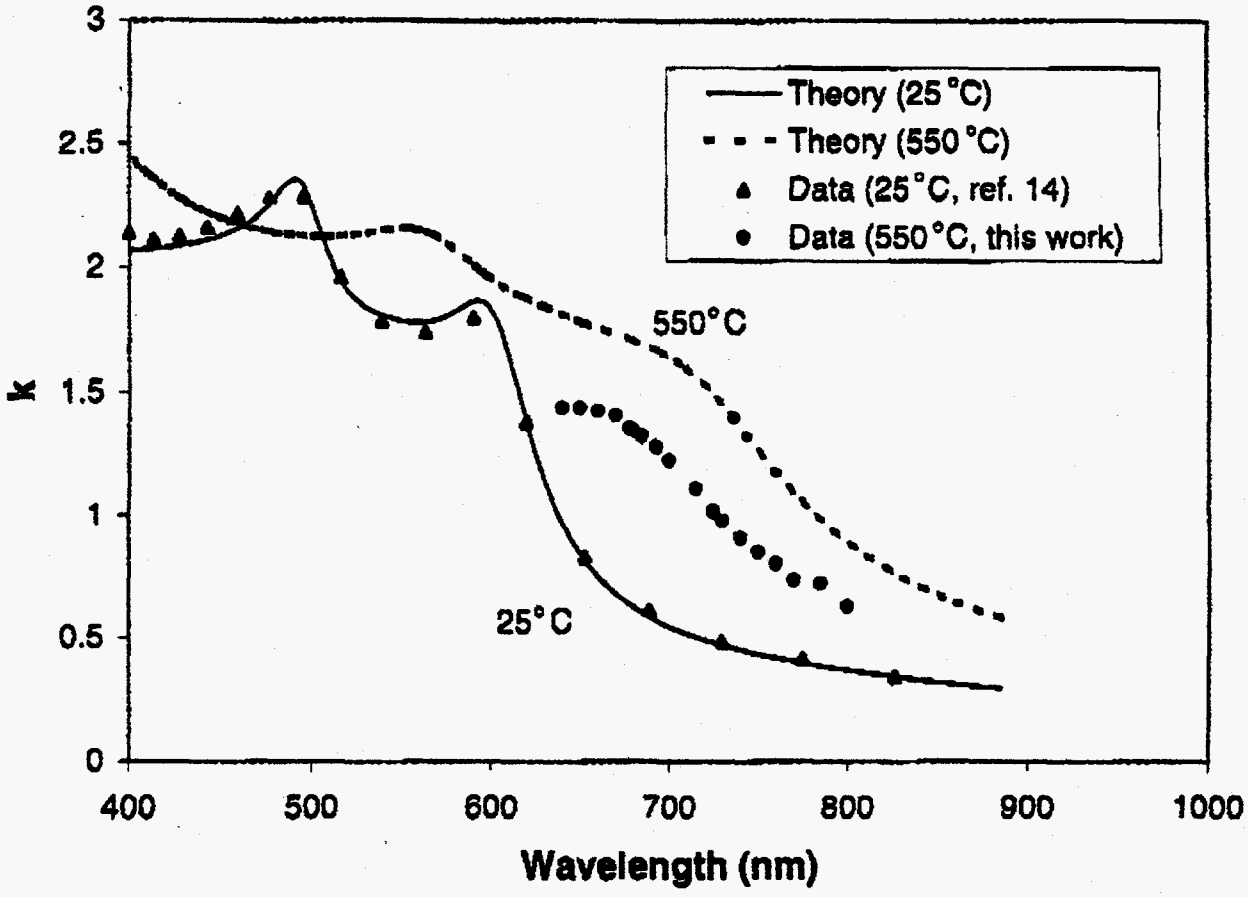

Figure 5(b). Imaginary part of the refractive index of GaSb.

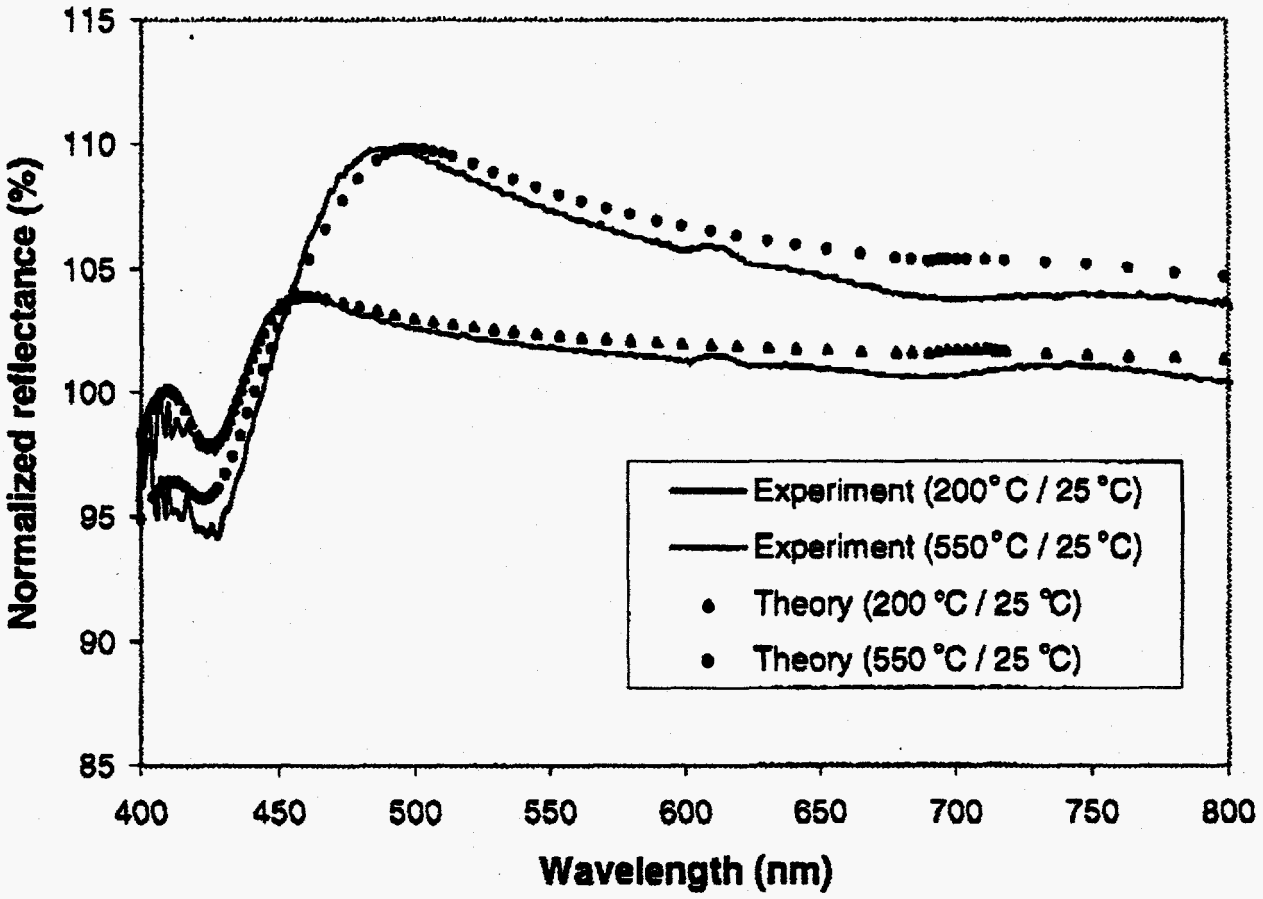

Figure 6(a). Theoretical and experimental reflectance spectra of GaAs as a function of temperature. The reflectance at elevated temperature is normalized to the reflectance at 25° C.

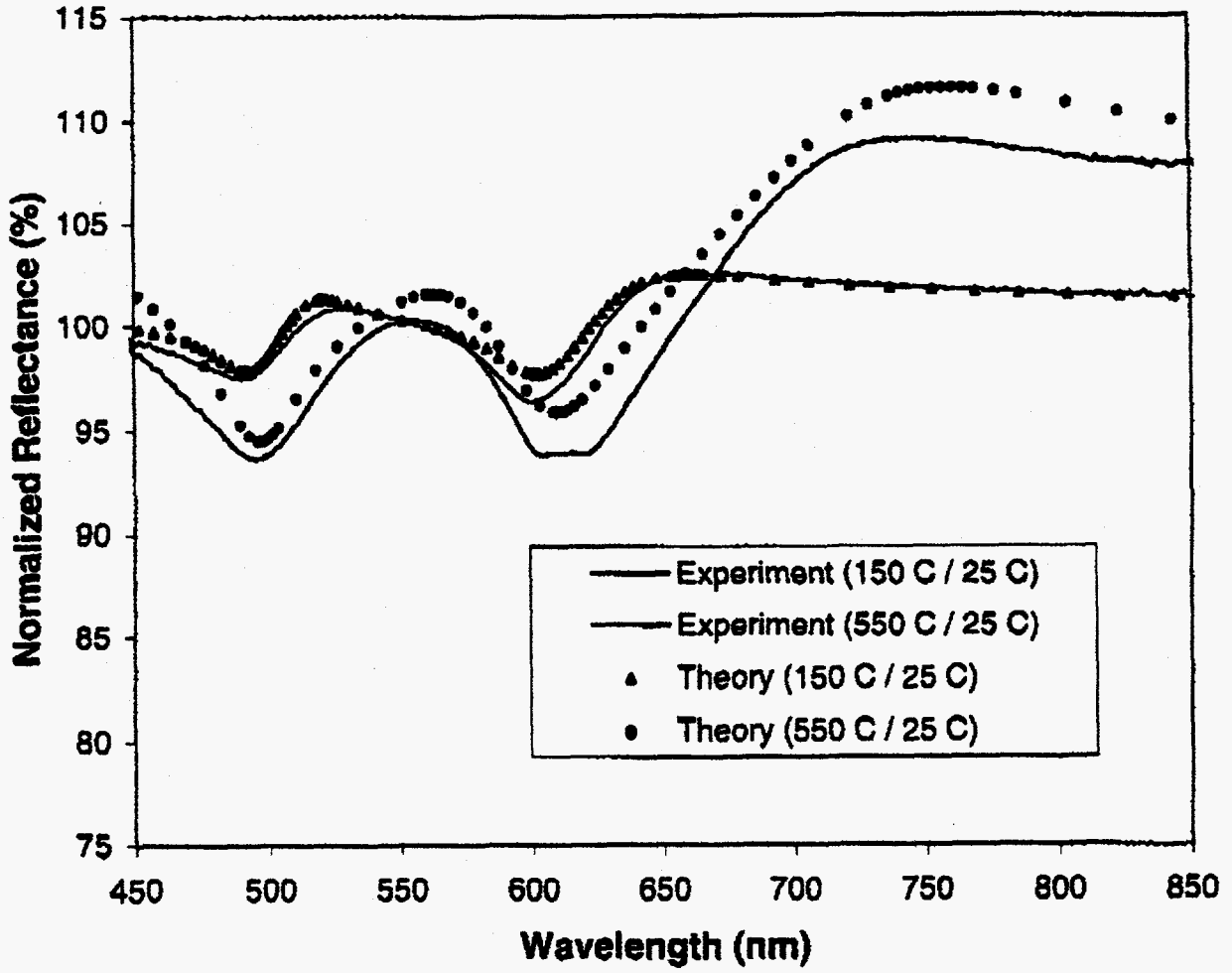

Figure 6(b). Theoretical and experimental reflectance spectra of GaSb as a function of temperature. The reflectance at elevated temperature is normalized to the reflectance at 25°C.

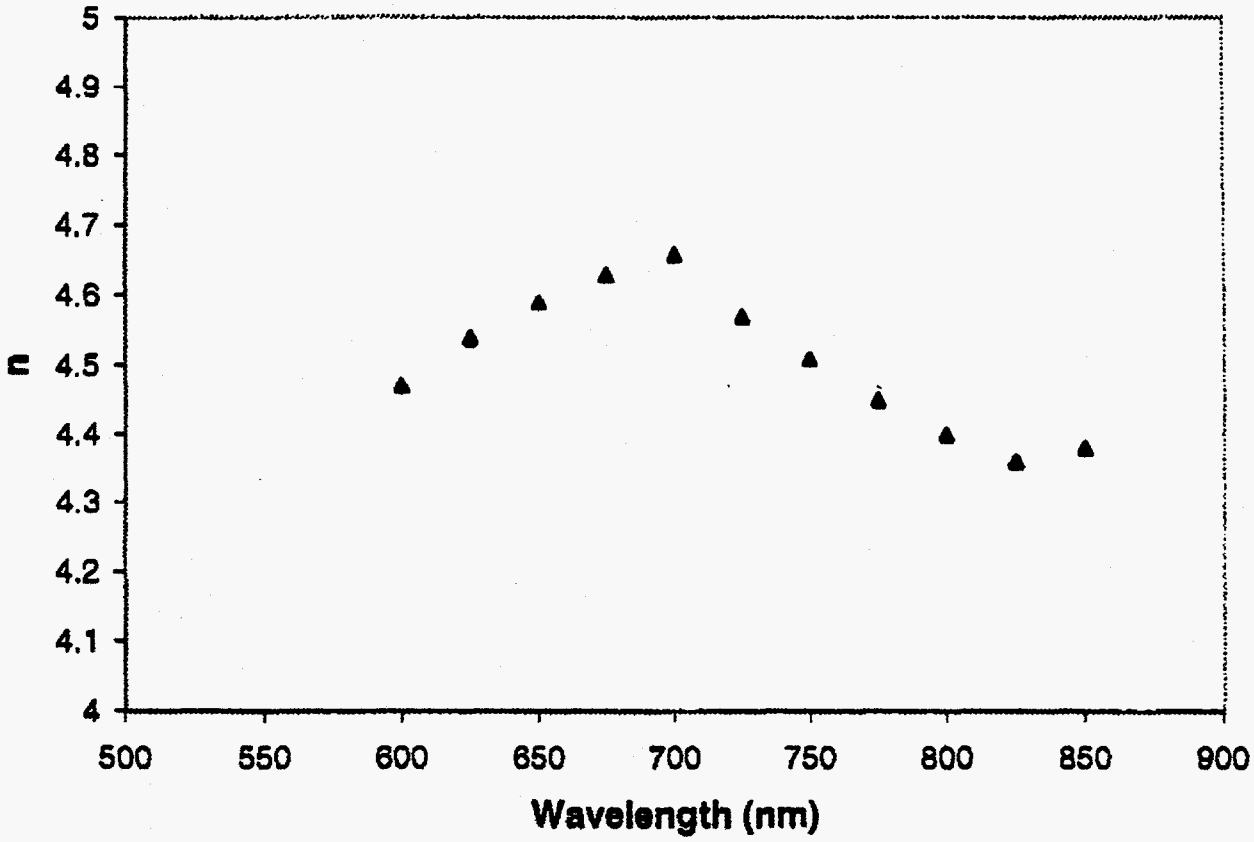

Figure 7(a). Real part of the refractive index for AlGaAsSb (bandgap = 1.2 μm at 25°C) at 550°C. Determined by reflectance of AlGaAsSb on GaSb (shown in Figure 3 for 800 nm).

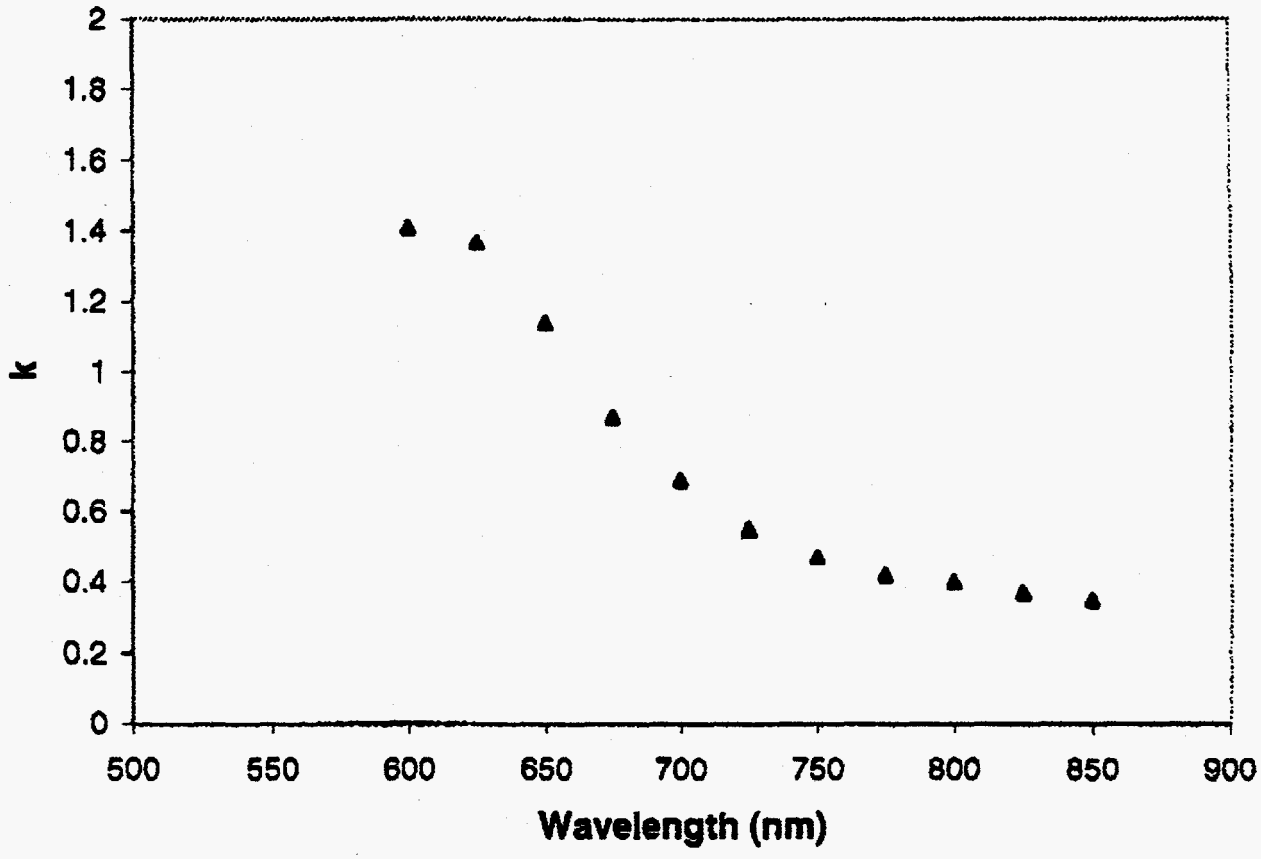

Figure 7(b). Imaginary part of the refractive index for AlGaAsSb (bandgap = 1.2 μm at 25°C) at 550°C. Determined by reflectance of AlGaAsSb on GaSb (shown in Figure 3 for 800 nm).

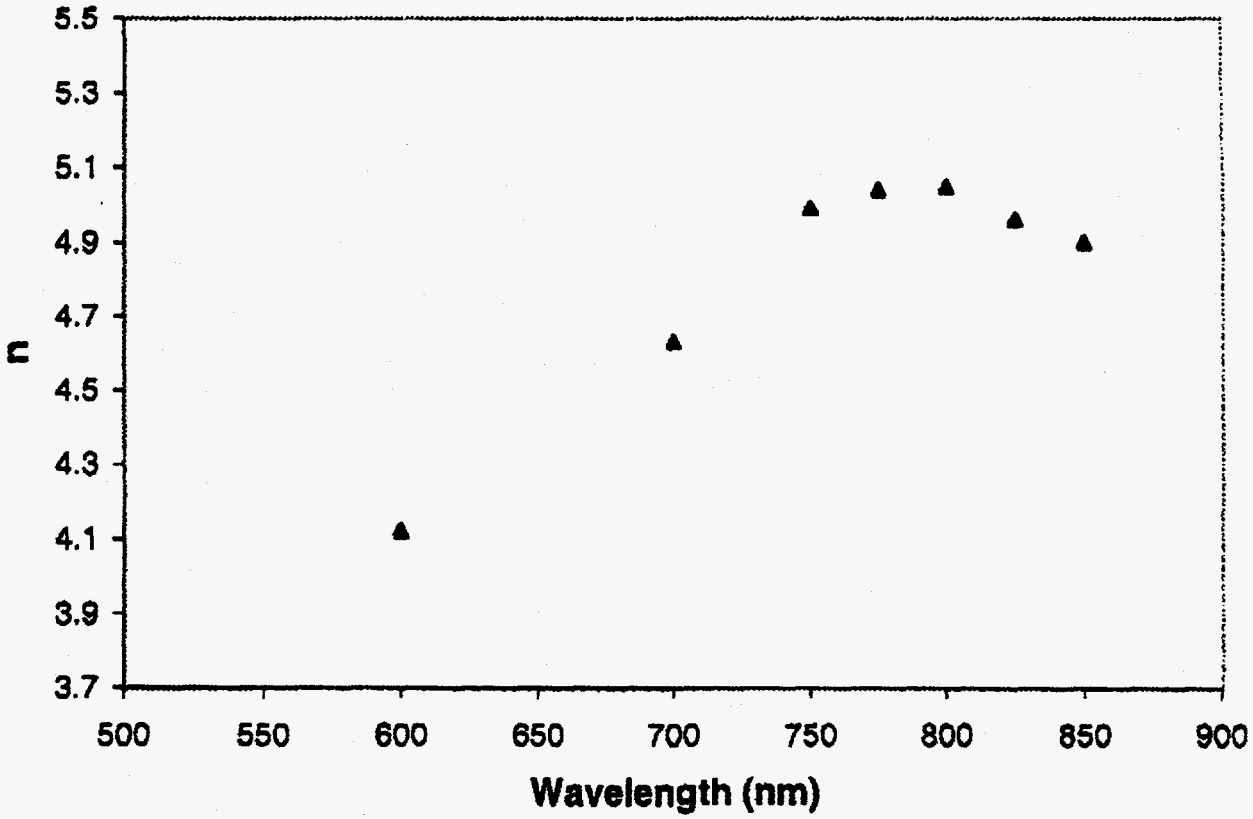

Figure 8(a). Real part of the refractive index of GaInAsSb (bandgap = 2.3 μm at 25°C) at 550°C. Extracted from the reflectance signal of GaInAsSb, as shown in Figure 3 for 800 nm.

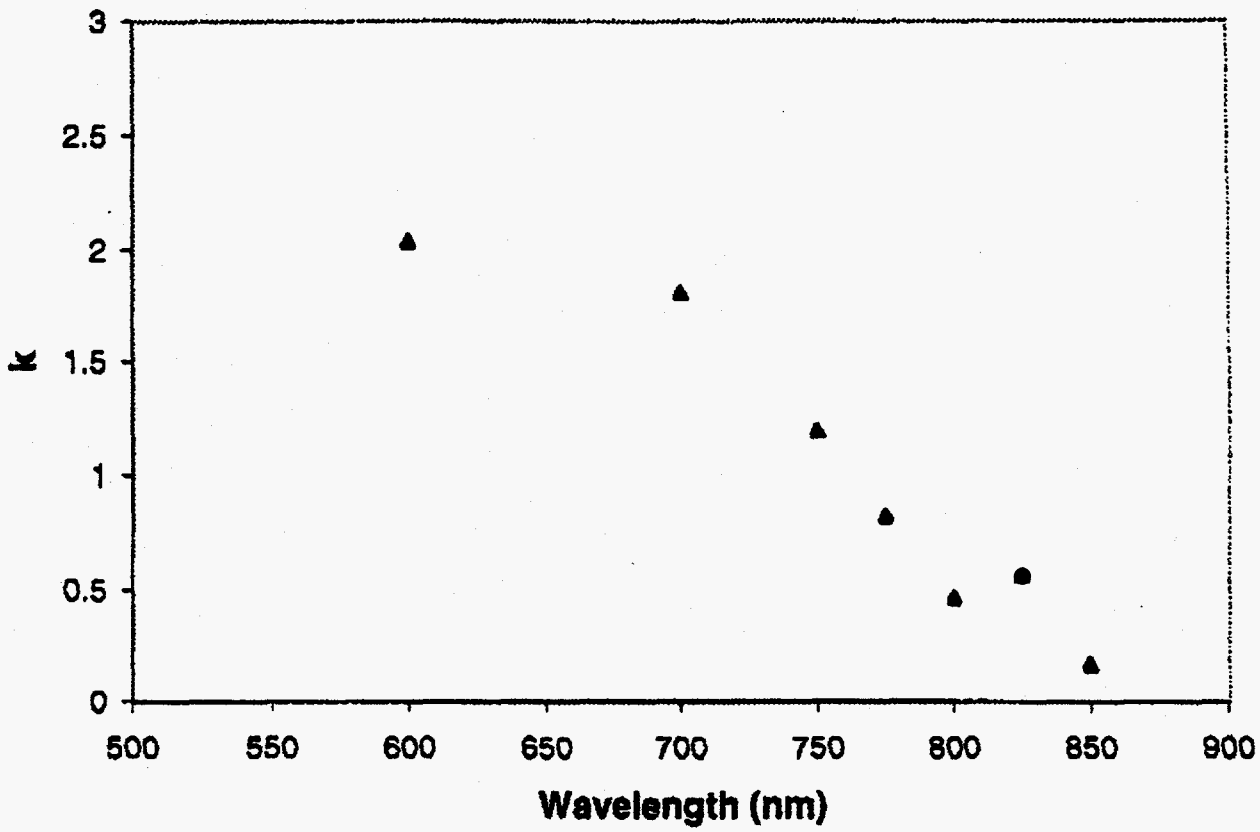

Figure 8(b). Imaginary part of the refractive index of GaInAsSb (bandgap = 2.3 μm at 25°C) at 550°C. Extracted from the reflectance signal of GaInAsSb, as shown in Figure 3 for 800 nm.

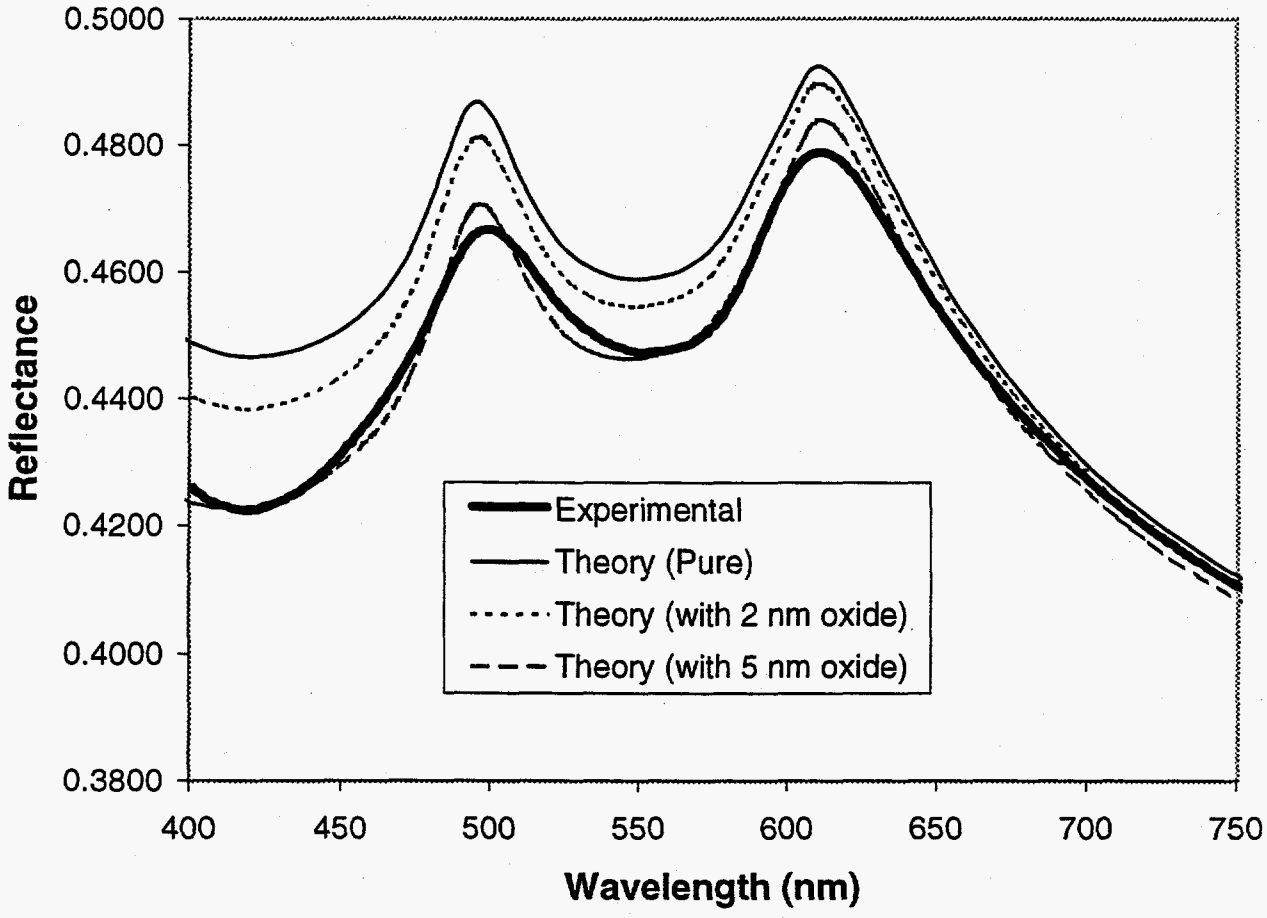

Figure 9. Theoretical and experimental reflectance spectra of GaSb substrates with oxide overlayers of various thickness.